

M Mantsinen et al

Controlling the Profile of Ion-Cyclotron-Resonant Ions in JET with the Wave-Induced Pinch Effect

Controlling the Profile of Ion-Cyclotron-Resonant Ions in JET with the Wave-Induced Pinch Effect

M.J. Mantsinen¹, L.C. Ingesson², T. Johnson³, V.G. Kiptily⁴, M.-L. Mayoral^{4,5},
S.E. Sharapov⁴, B. Alper⁴, L. Bertalot⁶, S. Conroy³, L.-G. Eriksson⁵,
T. Hellsten^{3,7}, J.-M. Noterdaeme⁸, S. Popovichev⁴, E. Righi^{9,10}, A.A. Tuccillo⁶

¹Helsinki University of Technology, Association Euratom-Tekes, Finland

²FOM-Rijnhuizen, Ass. Euratom-FOM, TEC, Nieuwegein, The Netherlands

³Euratom-VR Association, Swedish Research Council, Stockholm, Sweden

⁴Association Euratom-UKAEA, Culham Science Centre, Abingdon, OX14 3DB, UK

⁵Association EURATOM-CEA sur la Fusion, CEA Cadarache, St. Paul lez Durance, France

⁶Associazione EURATOM-ENEA sulla Fusione, Frascati, Rome, Italy

⁷EFDA-JET CSU, Culham Science Centre, Abingdon, United Kingdom

⁸Max-Planck IPP-EURATOM Assoziation, Garching, Germany

⁹EFDA CSU-Garching, Garching, Germany

¹⁰Present Address: European Commission, Brussels, Belgium

“This document is intended for publication in the open literature. It is made available on the understanding that it may not be further circulated and extracts or references may not be published prior to publication of the original when applicable, or without the consent of the Publications Officer, EFDA, Culham Science Centre, Abingdon, Oxon, OX14 3DB, UK.”

“Enquiries about Copyright and reproduction should be addressed to the Publications Officer, EFDA, Culham Science Centre, Abingdon, Oxon, OX14 3DB, UK.”

ABSTRACT

Experiments on the JET tokamak show that the wave-induced pinch effect in the presence of toroidally asymmetric waves can provide a tool for controlling the profile of ion-cyclotron-resonant ^3He ions. Direct evidence for the wave-induced pinch has been obtained from the measured γ -ray emission profiles. Concurrent differences in the excitation of Alfvén eigenmodes (AEs), sawtooth stabilisation, electron temperatures and fast-ion stored energies are observed. The measured location of AEs and the γ -ray emission profiles verify the fast ion radial gradient as the driving term for AEs.

PACS numbers: 52.50.Qt, 52.55.Fa, 52.55.Pi

Ion-cyclotron-resonance-frequency (ICRF) heating of ^3He minority ions is foreseen as one of the main auxiliary heating methods to be used in next-step burning plasma experiments. On the JET tokamak, ^3He minority heating is a well-established heating method that has been used in a wide variety of experiments [1-4]. In particular, its potential for ion heating has been demonstrated in deuterium-tritium plasmas on JET [2, 3]. This Letter reports first experiments performed on JET towards controlling the radial profile of ICRF-heated ^3He minority ions with the ICRF-induced pinch effect [5, 6]. The development of profile control methods is important for the optimization of ICRF heating and current drive in present-day and future tokamak experiments. In contrast to profile control by varying the ICRF resonance position or by inducing radial transport of resonant passing ions [7, 8], the present method is based on inducing radial transport of resonant trapped ions with toroidally directed waves and can be used irrespective of the resonance location.

The ICRF-induced pinch arises due to modifications in the toroidal angular momentum of the resonating ions, $P_\phi = mRv_\phi + Ze\psi_p$, when these ions are accelerated by toroidally directed waves [5]. Here, m and Ze are the ion mass and charge, respectively, R is the major radius, ψ_p is the poloidal flux related to the tokamak minor radius a as $r/a \approx \sqrt{\psi_p(r)/\psi_p(a)}$, and v_ϕ is the ion velocity component in the toroidal direction. These modifications give rise to radial transport of fast resonating ions and modify their orbits in a fundamental way [9, 10]. In the case of an inward pinch (i.e. for waves propagating in the direction of the plasma current), the turning points of the trapped ions move towards the midplane as they are heated. If the turning points meet in the midplane, the orbit is de-trapped into a passing orbit. This mechanism produces dominantly co-current passing orbits that will be shifted to the low field side due to ∇B and curvature drifts [10]. In the case of an outward pinch (i.e. for waves propagating in the counter-current direction), the standard trapped orbits dominate and the turning points of the orbits move outwards along the resonance layer. Thus, an inward pinch tends to improve the confinement of the fast ions, whereas the fast ion confinement tends to degrade for an outward pinch. The ICRF-induced pinch also modifies the current driven by the resonating ions [9, 11].

The ICRF-induced pinch of resonating ions was observed for the first time in experiments with hydrogen minority heating in JET [6]. Differences in the fast-ion-related quantities such as in

the sawtooth behavior, Alfvén eigenmode activity and line-integrated fast proton distribution functions were observed and explained successfully in terms of the ICRF-induced pinch predicted by theory. Later, the ICRF-induced pinch has been found to play an important role during high-power hydrogen minority heating with toroidally asymmetric waves in a variety of experimental conditions on JET [12-14]. However, no direct measurements have been available so far for the radial fast ion profiles during ICRF heating in the presence of toroidally asymmetric waves.

In the experiments reported in this Letter, information on the radial profile of fast ^3He ions was obtained from γ -ray emission during high-power ^3He minority heating. The observed γ -ray emission was due to the nuclear reaction $^{12}\text{C}(^3\text{He},p\gamma)^{14}\text{N}$ between ICRF-accelerated ^3He ions and carbon, which is the main impurity species in JET plasmas. The measurements were made in two 3.45 T/1.8 MA ^4He plasmas shown in Fig. 1. In both discharges up to 7.2 MW of ICRF power was tuned to a ^3He minority resonance at $R \approx 2.8$ m using a frequency of 37 MHz. In discharge 54239 the waves were launched in the co-current direction ($+90^\circ$ phasing), while in discharge 54243 the waves were in the counter-current direction (-90° phasing). A puff of 1.5×10^{19} ^3He ions was added before the application of ICRF power (Fig. 1a). The ^3He concentration, $n(^3\text{He})/n_e$, is estimated to be about 1-2%. As can be seen in Fig. 1, for the same ICRF power (up to $t = 10$ s) and plasma density, $+90^\circ$ phasing gives rise to a higher plasma stored energy W_{DIA} and electron temperature T_e than -90° phasing.

Information on the radial profile of the fast ^3He was obtained from γ -ray emission profiles measured with the JET neutron and gamma-ray profile monitor [15]. The profile monitor has two cameras that view the plasma along 19 lines-of-sight in the poloidal plane and was set up to measure γ -rays in the energy range 1.8-6 MeV. The γ -ray profile data, integrated over the quasi-steady-state phase of the discharges, was tomographically reconstructed using the tomography method [16] routinely used in tomography applications in JET. As can be seen in Figs 2 and 3, there are profound differences in the γ -ray emission profiles for the two phasings. The γ -ray emission for $+90^\circ$ phasing is stronger and spread out on the low-field side of the ^3He minority resonance layer at $R \approx 2.8$ m, whereas the γ -ray emission for -90° phasing is weaker and spread along the ^3He minority resonance layer. These differences in the overall shapes of the measured γ -ray emission profiles prevail when the regions of uncertainty, determined using the technique of varying reconstruction parameters within a reasonable range as described in Refs [15, 16], are taken into account (Fig. 3). Gamma-ray energy spectra measured with another device, a BGO scintillation detector [15] reveal that the γ -ray emission from this discharge is mainly due to the nuclear reaction $^{12}\text{C}(^3\text{He}, p\gamma)^{14}\text{N}$. This reaction between fast ^3He ions and carbon can take place when the energy of the fast ^3He ions exceeds ≈ 1.3 MeV [15]. The carbon concentration, deduced from visible spectroscopy was similar, $n_c/n_e \approx 5$ -10%, in both discharges.

In Fig. 3 the radial profiles of the γ -ray emissivity, calculated using the ICRF modeling code SELFO [10, 17] and the γ -ray modeling code GAMMOD [15], are also displayed. SELFO calculates the wave field and the ion distribution function with the three-dimensional orbit-

averaged Monte-Carlo model self-consistently, taking into account the effects due to finite orbit widths and the wave-induced pinch. The ^3He ion distribution functions given by SELFO have been used in GAMMOD to calculate the γ -ray emissivity due to the $^{12}\text{C}(^3\text{He}, p\gamma)^{14}\text{N}$ reaction, assuming radially constant $n(^{12}\text{C})/n_e$. As can be seen in Fig. 3, the calculated γ -ray emission profiles show similar trends as the reconstructed profiles: a maximum emissivity around the ^3He minority resonance layer for discharge 54243 with -90° phasing and a broader profile for discharge 54239 with $+90^\circ$ phasing. The modeling thus confirms that the differences in the measured γ -ray profiles are consistent with

- (a) an inward pinch of resonating ^3He ions with $+90^\circ$ phasing which produces, due to de-trapping of resonant ion orbits, a significant number of high-energy non-standard passing ions on the low field side of the resonance [10], and
- (b) an outward pinch of resonating ^3He ions with -90° phasing which produces a smaller number of high energy ions, which are predominantly trapped ions with turning points located along the resonance.

According to SELFO, the collisional power transfer from fast ^3He ions to the background electrons inside $r/a = 0.5$ is about 20% higher for $+90^\circ$ phasing. This is consistent with the 10% higher T_e for $+90^\circ$ phasing (Fig. 1d). The ion temperature T_i is about 40-50% lower than T_e in both discharges, consistent with predominant electron heating. Due to the low ^3He concentration, a significant number of fast ^3He ions have energies above the critical energy [18] of ≈ 200 keV for equal ion and electron power partition. SELFO gives a perpendicular fast ion energy of 0.35 MJ and 0.45 MJ for -90° and $+90^\circ$ phasing, respectively. These values are within the error bars of the perpendicular fast ion energies of $\approx 0.30 \pm 0.15$ MJ and 0.50 ± 0.15 MJ deduced from the measured data as $W_{\perp, \text{fast}} = 2(W_{\text{DIA}} - W_{\text{th}})/3$. Here, W_{th} is the thermal stored plasma energy estimated from the measured plasma densities and temperatures.

Further confirmation for the different radial profiles of the resonating ^3He minority ions comes from the sawtooth behavior and the excitation of Alfvén eigenmodes (AEs) as in the earlier ICRF-pinch experiments on JET [6, 12]. The sawtooth period τ_{saw} deduced from soft x-ray data is about two times longer with $+90^\circ$ phasing in the main ICRF heating phase (cf. Fig. 1e), indicating a higher fast ion pressure inside the $q = 1$ surface for this phasing. According to SELFO, the fast ion stored energy inside the sawtooth inversion radius is indeed about 30% higher in the case of the inward pinch ($+90^\circ$ phasing). Observation of AEs driven by fast ions can provide information on the radial profile of the fast ion population since the fast ion instability drive is proportional to the radial pressure gradient of the fast ions at the location of the mode when $n\omega_{\text{fast}} > \omega$. Here, n is the toroidal mode number, ω is the mode frequency, and ω_{fast} is the fast-ion diamagnetic frequency which is proportional to the radial gradient of the distribution of energetic ions and increases with their effective tail temperature [19]. The AE activity was measured with magnetic pick-up coils from $t = 6.5$ s to $t = 10.5$ †s. While no AE activity was

observed with -90° phasing, both toroidal and elliptical AEs were observed with $+90^\circ$ phasing. The TAEs and EAEs have frequencies in the range of 150-250 kHz (Fig.4(a)) and 325-450 kHz, respectively, and their frequencies follow the Alfvén scaling $f \propto n_i^{-1/2}$ with the ion density.

Analysis of soft x-ray data shows that the $n = 1$ TAE, with a frequency of 193 kHz and a very high amplitude of up to $\delta B \approx 10^{-6}$ T at the plasma edge, is a radially-extended coherent mode with a width of 35-40 cm in the vertical direction (Fig.4(b)). This agrees well with the results from the ideal MHD code MISHKA1 [20] for the $n = 1$ TAE. As shown in Fig.3, the location of the $n = 1$ TAE coincides with the location of the maximum radial gradient of the fast ions, which confirms the theoretical prediction that the fast ion radial gradient provides the driving term for TAE. Around the measured mode location, the dimensionless fast ion pressure gradient $|R_0 \nabla \beta_{\text{fast}}|$, which is a measure of the energetic ion instability drive, is estimated with SELFO to be about 0.02-0.03 and thus close to values expected in next-step burning plasma experiments.

It should be noted that TAEs shown in Fig.4 are the first TAEs observed during ^3He minority heating on JET. There are two factors that contribute to this observation. Firstly, in earlier JET experiments with ^3He minority heating larger (5-10%) ^3He concentrations were routinely used in order to maximize ion heating. Secondly, for a given plasma electron density and ion temperature, the ratio of the Alfvén velocity to the thermal velocity of ions is higher in ^4He plasmas, as used in these experiments, than in standard D plasmas. Consequently, the ratio of thermal ion Landau damping in ^4He plasma to that in D plasma is as small as $\approx 2^{3/2} \exp[-(9\beta_i)^{-1}]$ where β_i is the thermal ion beta of D plasma, and therefore, the excitation of TAEs is easier in ^4He than in D.

To summarize, for the first time direct experimental evidence for the ICRF-induced pinch of the resonating ^3He ions has been obtained on JET from the measurements of γ -ray emission profiles during high-power ^3He minority heating. The ICRF-induced pinch arises due to absorption of wave angular momentum by the resonating ions in the presence of toroidally asymmetric ICRF waves [6]. Additional verification is obtained from differences in the AE excitation, sawtooth activity, electron temperatures and fast ion stored energies. Modeling with the ICRF code SELFO [10, 17] confirms that the observations are indeed consistent with the ICRF-induced pinch of ^3He minority ions predicted by theory. While the ICRF-induced pinch of hydrogen minority ions has been reported before [6], results reported in this Letter show for the first time that the ICRF-induced pinch can significantly modify the spatial distribution of fast ions and fast-ion related quantities including the ICRF power deposition during ^3He minority heating. With waves launched predominantly in the co-current direction, a higher radial gradient of fast ions is obtained at a higher fast ion energy content than with waves in the counter-current direction. These results are of importance for the optimization of ICRF heating and current drive in present-day tokamaks and future burning plasma devices. The ICRF-induced pinch could be used alone, or in conjunction with other methods such as varying the resonance location(s), ICRH power and the concentration of heated species, to affect the radial fast ion profile during ICRH heating. The experiments

reported in this Letter have also provided the first measurement of the radial profile of the ICRF-accelerated ions in the presence of AEs excited by these ions on JET. The radial location of the AEs is found to coincide with the location of the maximum gradient of the γ -ray emission profiles, which verifies the theoretical prediction [19] that the fast ion radial gradient provides the driving term for AEs.

This work has been performed under the European Fusion Development Agreement. The work carried out by UKAEA personnel was partly funded by the UK Department of Trade and Industry and EURATOM.

REFERENCES

- [1] The JET Team (presented by D.F.H. Start), Plasma Physics and Controlled Nuclear Fusion Research (13th IAEA Conference, Washington, 1990) (IAEA, Vienna, 1991) Vol. 1, 679.
- [2] D.F.H. Start et al., Phys.Rev. Lett. 80, 4681 (1998)
- [3] D.F.H. Start et al., Nucl. Fusion 39, 321 (1999)
- [4] M.J. Mantsinen et al., in Radio Frequency Power in Plasmas (13th Topical Conference, Annapolis, 1999) (AIP, New York, 1999) 120.
- [5] L. Chen, J. Vaclavik and G. Hammett, Nucl. Fusion 28, 389 (1988).
- [6] L.-G. Eriksson et al., Phys. Rev. Lett. 81, 1231 (1998).
- [7] C.S. Chang, June-Yub Lee, and H. Weitzner, Phys. Fluids B 3, 3429 (1991).
- [8] K.H. Finken et al. Phys. Rev. Lett. 73, 436 (1994).
- [9] T. Hellsten, J. Carlsson, and L.-G. Eriksson, Phys. Rev. Lett. 74, 3612 (1995).
- [10] J. Hedin, T. Hellsten, L.-G. Eriksson, and T. Johnson, Nucl. Fusion (to be published).
- [11] J. Carlsson, T. Hellsten, J. Hedin, Phys. Plasmas 5, 2885 (1998).
- [12] M.J. Mantsinen et al., Nucl. Fusion 40, 1773 (2000).
- [13] F. Nguyen et al., in Proceedings of 28th EPS Conference on Controlled Fusion and Plasma Physics, Funchal, 2001, Europhysics Conference Abstracts Vol. 25 A (European Physical Society, Geneva, 2001) 781.
- [14] O. Sauter et al., Phys. Rev. Lett. 88, 105001 (2002).
- [15] V. Kiptily et al., Nucl. Fusion (to be published).
- [16] L.C. Ingesson et al., Nucl. Fusion 38, 1675 (1998).
- [17] Hedin, J., Hellsten, T., Carlsson, J., in Theory of Fusion Plasmas (Joint Varenna-Lausanne Int. Workshop Varenna, 1999), (Editrice Compositori, Bologna, 1998) 467.
- [18] T.H. Stix, Plasma Physics 14, 367 (1972).
- [19] W. Kerner et al., Nucl. Fusion 38, 1315 (1998).
- [20] A.B. Mikhailovskii, G.T.A. Huysmans, W. Kerner, S.E. Sharapov, Plasma Phys. Rep. 23, 844 (1997).

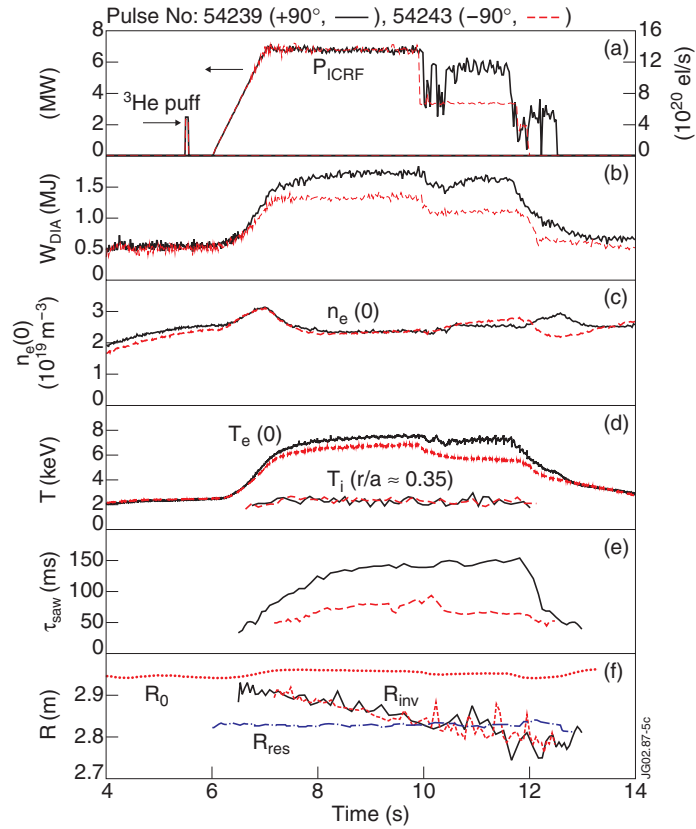


Figure.1: (a) ICRF power and ${}^3\text{He}$ puff, (b) total plasma diamagnetic stored energy, (c) electron density, (d) electron and ion temperatures, (e) sawtooth period determined from soft x-ray emission and (f) major radii of the sawtooth inversion radius, ${}^3\text{He}$ ion resonance layer and magnetic axis for two 3.45T/1.8 MA JET discharges in ${}^4\text{He}$ with ${}^3\text{He}$ minority heating using $+90^\circ$ and -90° phasings of the ICRF antennas.

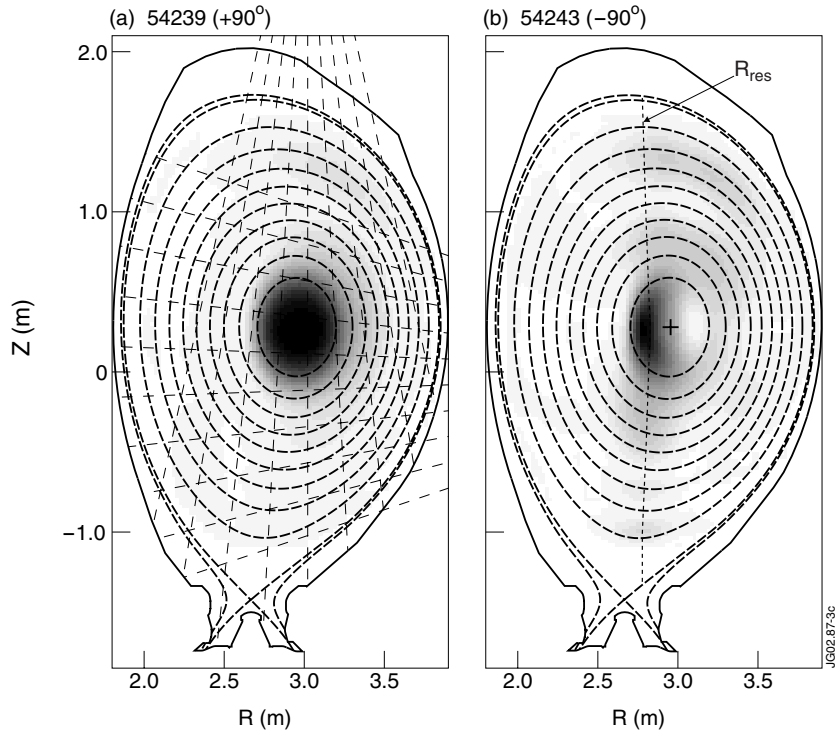


Figure.2: Contour plots of the reconstructed γ -ray emission profile, normalized to the peak emissivity. The lines-of-sight of the neutron profile monitor are shown in (a) and the ICRF resonance location in (b).

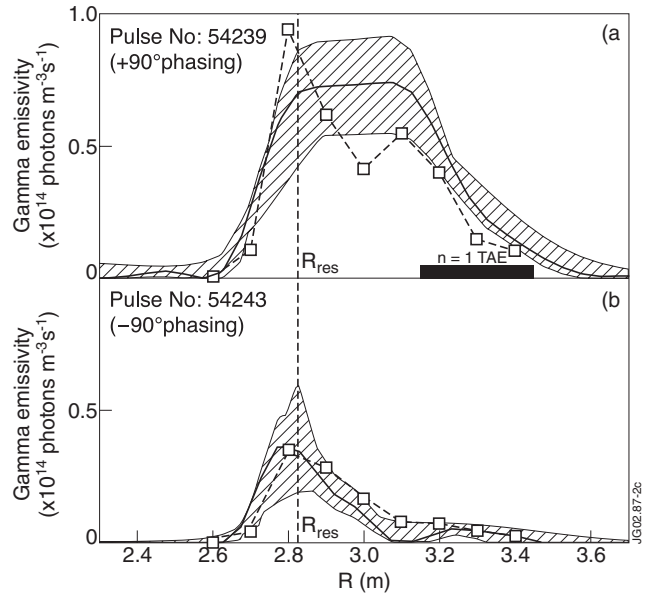


Figure.3: Reconstructed local γ -ray emissivity (solid line) together with the region of uncertainty (hatched region) and the calculated γ -ray emissivity (a.u., dashed line) along the midplane. In (a), the location of the $n = 1$ TAE, shown in Fig. 4b along the vertical direction, is also displayed mapped on the major radius coordinate.

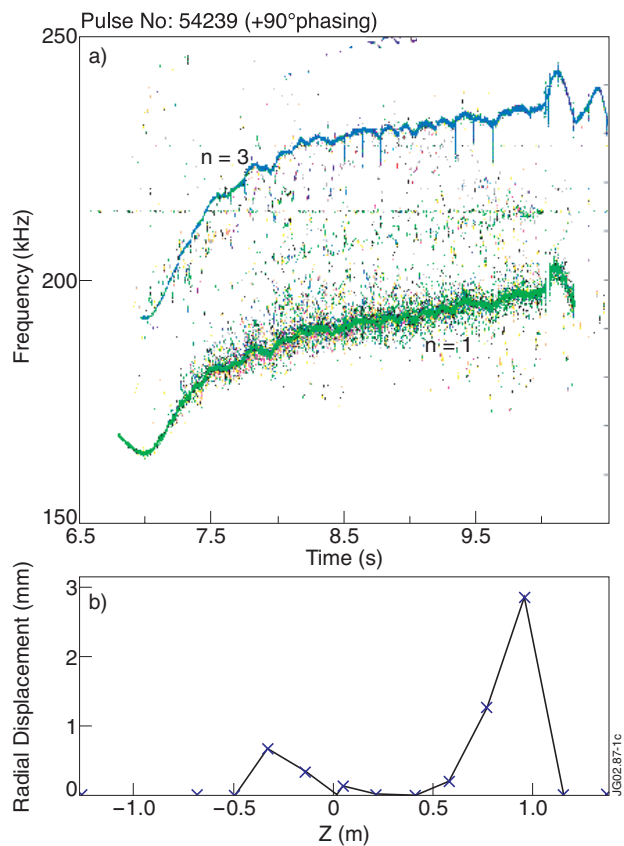


Figure.4: (a) Magnetic fluctuation spectrogram in the frequency range 150-250 kHz and (b) radial displacement of the $n = 1$ TAE along the vertical direction for discharge 54239. The magnetic axis is at $Z \approx 0.28$ m.